ORIGINAL RESEARCH ARTICLE

Lead Recovery From PbO Using Hydrogen as a Reducing Agent

A. RUKINI, M.A. RHAMDHANI, G.A. BROOKS, and A. VAN DEN BULCK

A systematic isothermal reduction study was carried out on pure PbO pellets using 15 pct H_2/85 pct N_2 gas. The reduction was carried out at 350 °C to 800 °C at different reaction times (30 minutes to 4 hours) with gas flowrate of 500 mL/min. The kinetics of the reaction were evaluated by measuring the mass change and applying kinetic models to the data. The results from microstructure observation showed that globular and non-wetting lead droplets form on the surface of PbO samples. The droplet's diameter was observed to increase with increasing temperature and reduction time. It was observed that this lead droplets layer, once covers the whole surface, appears to reduce the overall reduction rate. The kinetics analysis showed that PbO pellet reduction is a diffusion-controlled process as supported by the SEM (scanning electron microscope) micrographs, samples' cross-section observation, and phase analyses using EDS (energy-dispersive spectrometry) and XRD (X-ray diffraction). The energy activation, E_a, was calculated for two temperature ranges, *i.e.*, 61 kJ/mol (for 350 °C to 450 °C) and 224 kJ/mol (for 600 °C to 800 °C), respectively. These results suggest that, in an industrial context, continued reduction process will require constant removal of lead product from the surface of the lead monoxide.

https://doi.org/10.1007/s11663-023-02745-0

I. INTRODUCTION

REDUCTION process of lead monoxide (PbO) to lead (Pb) is a great importance in the lead industries. The detailed understanding of PbO reduction is not only important in the context of lead recovery from primary source, but also essential for further understanding and application of lead recovery from complex lead compound systems (*i.e.*, lead containing slag) and other secondary resources. The existing lead production technologies either through indirect smelting (*i.e.*, lead blast furnace) or through direct smelting (*i.e.*, Isasmelt, Outotec-Ausmelt, Kivcet, Kaldo, SKS, and QSL) involve the use of oxides burden in the form of PbO or PbO-containing raw materials. In the past 5 years (2016–2020), approximately 12,000 tonnes of lead produced globally, with more than half was sourced from secondary resources which made lead as one of the highly recycled metals.[1] However, all of the existing routes for the production of lead in the lead industries use carbon-based reductant (including methane) for the reduction process.

Amidst of decarbonization effort in metal production industries, researchers have been exploring and maximizing the potential of carbon-alternative reductants in the last few decades. Hydrogen is one of the alternative candidates to reduce and replace carbon usage for the lead production as it is thermodynamically favorable to be utilized as reducing agent for lead oxide reduction. Hence, the use of hydrogen-based reductant is promising to be utilized in some of the lead production technologies such as Isasmelt, Outotec-Ausmelt, Kivcet, and Lead Blast Furnace (LBF). For instance, hydrogen can potentially be injected into the melt bath through submerge lance in the Isasmelt and Outotec-Ausmelt reactor or can be injected in a lead blast furnace through the middle tuyeres for the reduction of the solid charge as it goes down the shaft with the coal/coke bed.

There are only limited studies in the open literatures on the detailed fundamental kinetic study of lead reduction from pure lead oxide or lead oxide mixtures using hydrogen.[2–5] Hydrogen in this context includes pure H_2 gas or H_2 gas mixture (with H_2O or inert gases, *i.e.* H_2-N_2, H_2-Ar). These key studies are summarized in Table I. Majority of the hydrogen reduction studies reported were related to the reduction of lead silicate materials[6–10] in the context of glass making as the compounds are important in the glass industry. The

A. RUKINI, M.A. RHAMDHANI, and G.A. BROOKS are with the Fluid and Process Dynamics (FPD) Group, Swinburne University of Technology, Melbourne, VIC 3122, Australia. Contact e-mail: ARhamdhani@swin.edu.au A. VAN DEN BULCK is with the Umicore, Corporate Research and Development, 2250, Olen, Belgium.
Manuscript submitted August 29, 2022; accepted February 5, 2023.
Article published online March 6, 2023.

experiments conducted in these studies aimed for lead deposition on the glass and not for the context of lead recovery. The study of kinetics of lead extraction from lead silicate system using hydrogen was also found to be limited. Pal *et al.*[2] conducted a study to analyze the relative magnitude of reduction rates at different slag interfaces (*i.e.*, slag gas, slag/refractory, slag/metal) when $PbO.SiO_2$ was subjected to hydrogen atmospheres at 900 °C. The analysis was carried out by observing the concentration profile using electron microprobe. The results concluded that the reaction mainly take place at slag/gas and slag/refractory interfaces. Additional remark of the study also mentioned that the presence of P_2O_5 was decreasing the reduction rate.

Culver *et al.*[3] carried out the kinetics study of PbO reduction by hydrogen at 475 °C to 775 °C and reported that the process was a diffusion-controlled. Their experiments were performed on a fixed bed PbO powder, and the kinetics were studied by measuring the amount of H_2O produced, in addition to measuring the Pb-PbO percentage with chemical assay in ammonium acetate. Culver *et al.* pointed out that further study is needed to understand the effect of water product on the kinetics. The study found that the addition of water vapor into hydrogen gas decreased the reduction rate compared to the rate in H_2-N_2 gas. Using their developed rate model, they pointed out that desorption of water (H_2O) was not the controlling step, rather they suggested that the adsorption of H_2 was the rate-controlling step. On the other hand, a study by Ivanov *et al.*[5] reported that the kinetics of PbO reduction in hydrogen atmosphere is controlled by a nucleation process. These experiments were also carried out on a fixed bed PbO powder, in which the amount of H_2O produced from reduction was used for kinetics analysis evaluation through a chromatography method. The kinetics itself was examined through the iso-conversion analysis approach. The main focus of Ivanov's study was to investigate the effect of different crystallographic form of PbO (between β-orthorhombic and α-tetragonal) on the kinetics behavior within the temperature range of 450 °C to525 °C where the polymorphic transition is expected to occur. The main finding from this work is that different crystallographic form does not affect the kinetics behavior.

The above-mentioned previous studies on hydrogen reduction of PbO were conducted using powder PbO sample and the kinetics evaluations were carried out using H_2O adsorption method and analyzed using an iso-conversional method. There are no studies reported in the literature on the reduction of lump and bulk PbO sample. Considering the importance of non-powder feed in industrial process (especially in lead blast furnace process), an investigation on the reduction of bigger size burden or pelletized sample is essential. Therefore, the current study intends to evaluate the kinetics and the micromechanism of PbO reduction in hydrogen atmosphere. In this study, pelletized PbO samples were reduced under hydrogen atmosphere (15 pct H_2-N_2) and the kinetics were measured *via* mass loss and analyzed through the implementation of solid–gas reaction isothermal kinetic models. This study also examines the morphological and microstructure evolution during the reduction. Overall, this study also provides fundamental information that is useful for the broader industrial lead production from PbO and Pb-containing secondary resources (*i.e.*, slag, tailing, sludge) using non-carbon reductant.

II. EXPERIMENTAL METHODOLOGIES

A. *Starting Material and Hydrogen Reduction Experiment Set-Up*

The starting material for the PbO reduction experiment was a high-purity PbO powder (> 99.9 pct) sourced from Sigma Aldrich, with an average mean size of 10 μm. Lead (Pb) droplets (with average diameter of 1 mm and purity > 99.9 pct) were also sourced from Sigma Aldrich for evaporation experiments. Each PbO pellet was made by weighing approximately 5 g of PbO powder, which then put and pressed into a steel die to form a pellet with diameter of 29.5 mm and thickness of 4.2 mm. The PbO powder was compacted using a hydraulic press with a force of 10 tonnes for 30 minutes.

In this study, systematic microstructure and kinetics analyses of solid-state PbO reduction in a mixture of 15 pct hydrogen-85 pct nitrogen (H_2/N_2) atmosphere were investigated. The main reason of using a low hydrogen concentration in the gas mixture is for a safe laboratory experimental procedure (reduce flammability of the gas mixture). Different concentration of hydrogen in the gas mixture may affect the reduction kinetics; however, the investigation of the effect of hydrogen concentration is beyond the current study. The mixture of ultra-high-purity hydrogen and nitrogen gas was sourced from Coregas. Isothermal reductions of PbO pellet at temperature range of 350 °C to 800 °C were carried out in a vertical resistance tube furnace (equipped with Mo_2Si heating elements) as shown in Figure 1. In anticipation of having liquid Pb generated during reduction, a special sample holder arrangement was adopted where a shallow crucible was equipped with nickel chromium wire net as shown in Figure 1 (inset). This would allow the sample to be suspended and readily react with the hydrogen in the atmosphere and at the same time let any possible lead liquid to drip down and contained in the crucible.

The temperature in the hot zone of the furnace was calibrated with a standard reference thermocouple and found to be accurate within ± 1 °C. For the experiment, the PbO pellet on the crucible was positioned in the cool zone before the furnace was sealed and ultrahigh-purity Argon was blown into the furnace chamber for 5 minutes to purge the air out. The furnace was then heated to the designated temperatures, then the H_2/N_2 gas mixture was flown into the furnace chamber with constant gas flowrate of 500 mL/min. The pedestal was then lifted up to position the pellet in the heat zone of the furnace and this was set to be the time zero for the reaction. The pellet was then let to react with the hydrogen in the gas for different reaction times (from 30 minutes to 4 h). To terminate the reaction, the furnace chamber was bleed with Ar gas to flush the hydrogen mixture out of the furnace chamber, then the

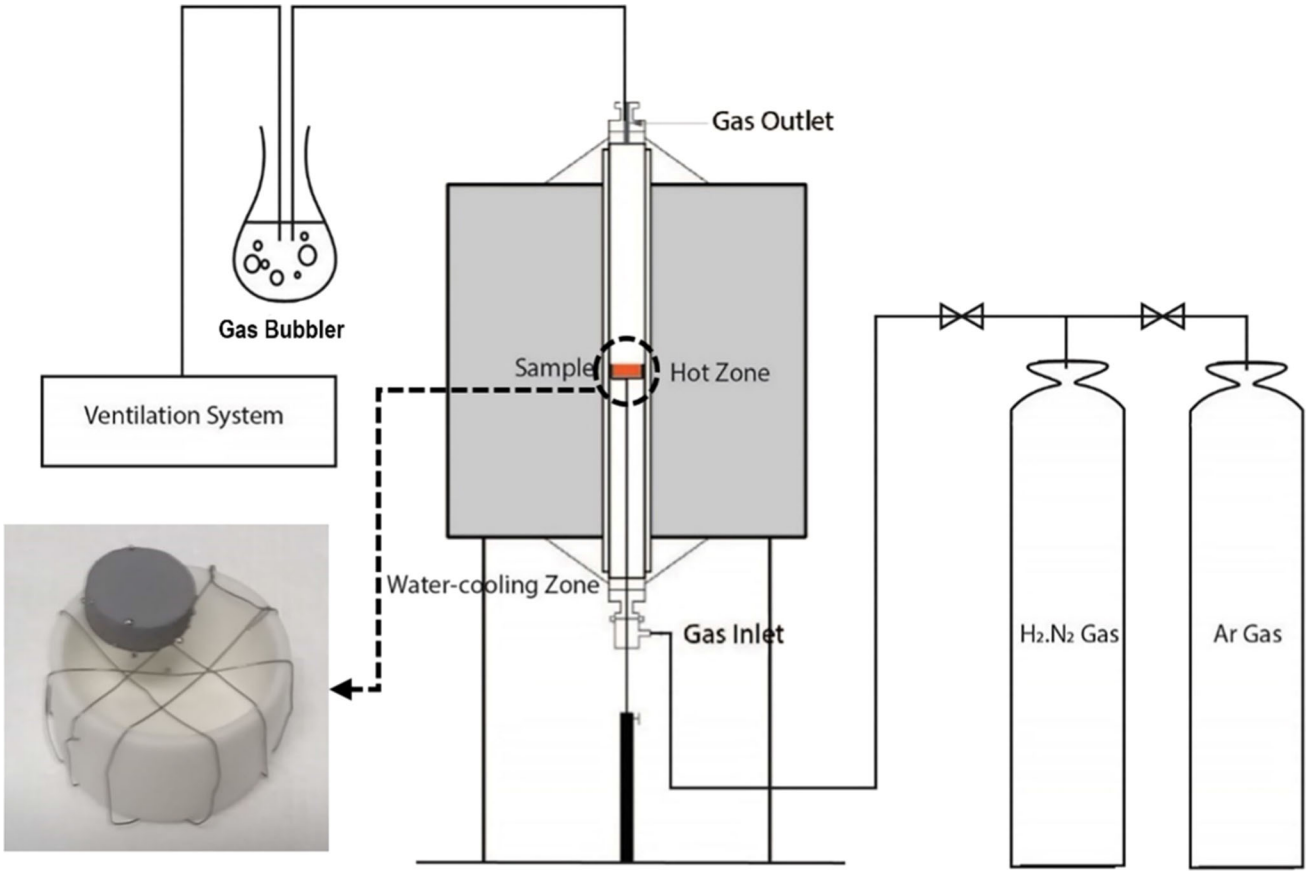

Fig. 1—A schematic of experimental apparatus consisting a vertical resistance tube furnace; with sample holder, gas, and ventilation systems; (inset) a crucible holder system equipped consisting a shallow alumina crucible with Ni–Cr wire net to hold the pellet sample and also functioning as a drain for liquid Pb.

pedestal was lowered to position the pellet in the cooling zone (cooled by circulating water and cold Ar gas) and let to rest for 30 minutes before the sample was extracted out from the furnace. The PbO pellet was weighed along with the crucible holder system both before and after the reduction experiments.

B. *Sample Characterizations and Kinetics Approach*

Scanning electron microscopy (SEM) observations and phase analyses using X-ray diffraction (XRD) technique were carried out on the PbO pellet samples before and after the experiments. The PbO surface morphology was examined using field emission SEM Zeiss Supra 40 VP, using accelerating voltage of 10 to 15 keV. The SEM instrument is equipped with an energy-dispersive X-ray spectroscopy (EDS) detector; hence, elemental characterizations were also carried out. The phases analysis was carried out using XRD Bruker D8 Advance (Cu Kα, $\lambda = 1.5418$ Å) with 2θ range from 5 to 80 deg. Quantitative phase analyses from XRD spectra were carried out using Rietveld quantification method through Profex® software.

The progress of PbO reduction by H_2-N_2 gas mixture was also tracked by measuring the mass loss of the pellet at particular time and temperature. The degree of reduction or extent of reduction at a particular time (α_t) was defined as the ratio of mass loss measured at that time (ΔW_t) with theoretical maximum mass loss (ΔW_{total}), see Eq. [1]. Here, m_t, m_i, and m_{total} are the mass at time t (g), at initial (g), and at maximum oxygen removal, respectively. It was assumed that the mass loss measured reflects the oxygen removal from PbO with neither substantial evaporation of raw material (PbO) nor product (Pb). While the final theoretical mass loss was defined as the total possible mass loss when all oxygen element is completely removed from PbO.

$$\alpha_t = \frac{\Delta W_t}{\Delta W_{total}} = \frac{m_i - m_t}{m_i - m_{total}} \quad [1]$$

The incorporation of α into a suitable model is useful for kinetics analysis and also to be used to determine the rate-controlling step and micromechanism. Models that represent the solid–gas reaction have been comprehensively explained.[11–13] The current work kinetics interpretation includes the fitting of experimental result data (α) into existing isothermal kinetics models which include nucleation models, reaction order models, geometrical contraction models, and diffusion models. The value of (R^2) from a linear regression of each model was evaluated and triangulated with the phase analysis and microstructure evolution observation to determine the micromechanism and possible rate-limiting step.

III. RESULTS AND DISCUSSION

A. *Starting Material Characterizations*

PbO is known to have two polymorph phases, namely PbO tetragonal (also known as litharge or red-PbO or α-PbO) and PbO orthorhombic (also known as massicot or yellow-PbO or β-PbO). The tetragonal α-PbO phase is stable at low temperature (room temperature) and can transform to orthorhombic β-PbO phase at temperature range of 486 °C to 489 °C.[14] Different transition temperatures, however, have been reported in the literature. Risold *et al.*[15] reported that the α-PbO to β-PbO polymorphic transition occurs between 488 °C and 530 °C, while Oka *et al.*,[16] based on a color change, reported the transition to occur above 500 °C.

Figure 2 shows the XRD analysis results, while Figure 3 shows the color/physical appearance of the raw PbO powder, PbO pellet, and heat-treated PbO pellet, as well as the SEM images of the pellet's surface. It can be seen from Figure 2 that the original PbO powder contained both the orthorhombic β-PbO and tetragonal α-PbO phases indicated by the presence of their peaks. However, after pellet making process, the intensity of tetragonal α-PbO peaks was found to increase which indicated an increase in the amount of the tetragonal α-PbO phase in the pellet. Visually, there was also distinguishable color change between the raw PbO powder, and the PbO pellet, as shown in Figure 3. This was confirmed by the Rietveld phase quantification analysis result shown in Table II. The raw PbO powder with reddish yellow color was confirmed through Rietveld quantification to contain approximately 89 pct and 11 pct of orthorhombic β-PbO and tetragonal α-PbO phases, respectively. After pelletizing, a color change from bright reddish yellow powder into dark red pellet could be observe, as shown in Figure 3. It appeared that the pelletizing process provides a constrain (mechanical force) to the orthorhombic β-PbO lattice which transforms it to the tetragonal α-PbO phase. The amount of the tetragonal α-PbO phase was found to increase from 11 to 36 pct after pelletizing.

A heat treatment of the PbO pellet was carried out in Ar gas at 500 °C for 1 h to investigate further the reversal of polymorphic transition. The color of the pellet was found to change to a brighter yellow post-heat treatment. The Rietveld quantification analysis showed that the amount of tetragonal α-PbO and orthorhombic β-PbO is 0.8 pct and 99.2 pct, respectively. It appeared that the thermal treatment transformed almost all of the PbO to its orthorhombic β-PbO phase. It is worth to note that orthorhombic β-PbO is stable at high temperatures, *i.e.*, above 500–530 °C. However, it appeared that the β-PbO when rapidly cooled down, the structure would stay as metastable orthorhombic β-PbO even at temperature of liquid helium.[13,14] It was reported that this metastable phase was able to persist for more than ten years at room temperature[13] and could be converted to α-PbO when stress was applied. Polymorphic transformation of α-PbO into β-PbO happened due to thermally induced process. On the other hand, the transformation of β-PbO into α-PbO that happened at room temperature is a mechanically induced transformation. The transformation was proposed by Soederquist and Dicknes[17] as a sublattice contraction and dilation as much as 13 pct along the (001) plane and as much as 18 pct along the (010) plane, respectively, which consume the least minimum energy. The information on the behavior of α-PbO and β-PbO phase before and after pelletizing process and after heat treatment, presented above, is important in the context of identifying the reduction mechanism as will be presented later in the mechanism Section in this paper.

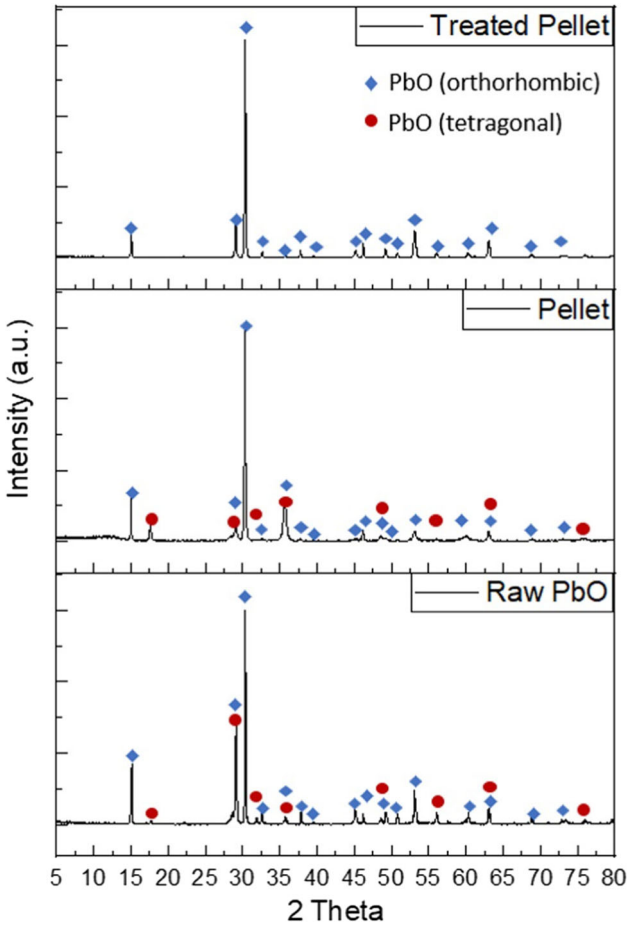

Fig. 2—X-ray diffraction spectra of the starting powder PbO, pelletized PbO, and heat-treated pellet (at 500 °C in Ar atmosphere for 1 h) indicating phase transformation between tetragonal α-PbO and orthorhombic β-PbO upon applying mechanical stress and heat treatment.

B. *Assessment of the Effect of PbO and Pb Evaporation Rates and Gas Flow Rates*

Initial tests were carried out to evaluate the rate of evaporation of PbO and Pb at high temperature conditions. These tests were carried out to check whether the PbO and Pb evaporation rates are negligible compared to the overall weight reduction during the reduction process. PbO pellets (~ 5 g each experiment) and Pb droplets (totalling 5 g each experiment) were heated at 700 °C in Ar atmosphere (flowrate of 500 mL/min) and held for different times. The results of the

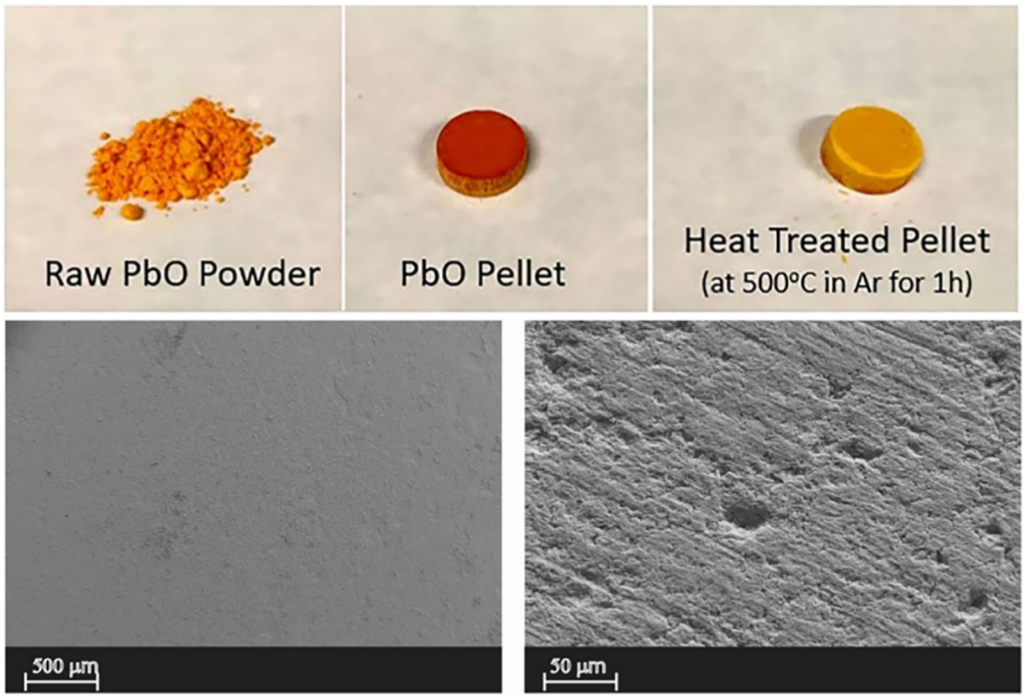

Fig. 3—Visual appearance of the starting PbO powder, pelletized PbO pellet, and heat-treated PbO (at 500 °C in Ar atmosphere for 1 h)—(top); SEM images of the surface of PbO pellet before reduction—(bottom).

evaporation tests of both PbO and Pb are given in Figure 4. To compare, the PbO reduction data under H_2-N_2 atmosphere at 700 °C were also plotted. It can be seen from Figure 4 that there were no significant mass changes of the PbO and Pb sample in Ar. The accumulation of PbO and Pb was calculated to be less than 0.5 pct of total weight reduction during reduction experiments; hence, it was confirmed that evaporation rates of PbO and Pb were negligible.

The effect of flowrate of H_2-N_2 was also investigated to check whether gas phase mass transfer might be controlling the reduction process. For this purpose, three different flowrates, *i.e.*, 300, 500, and 700 mL/min, were tested for the PbO reduction at 700 °C, and the results are presented in Figure 5. It can be seen that the discrepancy of weight loss using different gas flowrate was relatively small and still within the deviation range. It can be concluded from this results that the reduction rate was independent of the gas flowrate, hence was not controlled by gas phase mass transfer, which was in agreement with previous studies.[3,5]

C. *Observation of the Surface of the Pellets*

Visual observation of the PbO pellets' surface after hydrogen reduction was carried out and the macrographs are presented in Figure 6. The most noticeable physical change observed on the PbO pellets after reduction was a color change from reddish yellow (Figure 3) into gray (Figure 6). For samples reduced at 400 °C, there were no lead droplets observable by naked eye. However, upon microscopy and XRD analyses, microdroplets of lead were found to form already at this temperature (as shown in Figure 7(a)). At 500 °C and 600 °C, many small lead droplets with few bigger droplets were observed. At higher temperatures (700 °C and 800 °C), significant amount of lead droplets was observed on the surface. Coalescence of smaller droplets forming bigger droplets is observed. At long reduction times, some of the lead droplets dripped into the crucible. At 800 °C and 3 h, it appeared that all the PbO reduced to Pb.

Systematic pellets' surface examinations were carried out using scanning electron microscopy. Figure 7 shows the secondary electron images of selected pellets surface reduced at 400 °C and 500 °C for 1 to 4 h. At higher magnification of ×10,000, it can be seen that fine lead seeds with average size of 0.5 to 1.5 μm were observed to form on the surface of pellets reduced at 400 °C (Figures 7(a) through (d)). Similar trend was also observed for PbO pellets reduced at 500 °C, and fine lead droplets with average size of 0.5 to 7 μm were observed at 1 to 2 h reduction time (Figures 7(e) and (f)). Bigger sizes of lead droplets with average size between 10 and 50 μm were observed at longer reduction time of 3 to 4 h (Figures 7(g) and (h)). There were evidences of droplets coalescence to form a few macrodroplets (visible by naked eye; millimeters in size) as shown in Figure 6.

Secondary electron images of the pellets' surface after reduction at 600 °C and 700 °C are presented in Figure 8. In the case of samples reduced at 600 °C, small lead droplets (with diameter less than 1 μm) uniformly covered the surface of PbO pellet even as early as 30 minutes reduction. With further reduction times, the smaller droplets started to coalesce, forming

Table I. Studies on the Kinetics of Lead Reduction from PbO and PbO Mixtures Using Hydrogen

Lead Compound	Reducing Agent	Main Purpose of the Study	References
$PbO.SiO_2$ Melts	20 pct to 62 pct H_2-N_2	analyzing the reaction rate of hydrogen reduction at different slag interfaces (*i.e.* slag/gas, slag/refractory, slag/metal)	Pal *et al.*[2]
Pure PbO Powder	H_2-N_2 and H_2-H_2O	investigation of the effect of PbO particle size and the effect of different H_2 mixture (*i.e.* $H_2.N_2$ and H_2-H_2O) on hydrogen reduction of PbO	Culver *et al.*[3]
Pb-55.5 At. Pct Bi	3 pct H_2-Ar	kinetics study of hydrogen reduction of PbO in liquid Pb-Bi eutectic (application for corrosion control)	Ricapito *et al.*[4]
Pure PbO Powder (Tetragonal and Orthorhombic)	Pure H_2	Investigation of the reduction kinetics of tetragonal and orthorhombic PbO	Ivanov *et al.*[5]
$PbO.SiO_2$ Glass	H_2—10^5 Pa	investigation of the glass conductivity after hydrogen reduction	Blodgett[6]
$PbO.SiO_2$ Glass	H_2—10^5 Pa	XPS studies on the mechanism of glass composition change after hydrogen reduction	Kannunikova *et al.*[7]
(50–55 Pct) SiO_2—(25–30 Pct) PbO—(5–10 Pct) Bi_2O_3—(5–10 Pct) (K_2O + Na_2O)—(0–5 Pct) (BaO + MgO)	H_2—10^5 Pa	XPS (x-ray photoelectron spectroscopy) study of microchannel plates compositions after hydrogen reduction	Yonggang et.al. [8]
66 Pct SiO_2—18 Pct PbO—8 Pct (Na_2O + K_2O)—5 Pct (MgO + BaO)—3 Pct Bi_2O_3	H_2—10^5 Pa	investigation of the effect of hydrogen reduction on the microchannel plate glass properties (*i.e.* surface resistivity)	Zhang *et al.* [9]
PbO Powder	pure H_2	determining the temperature at which the reaction between PbO and H_2 started to take place	Gallo [10]

Table II. Rietveld Refinement Phase Quantification Results of the Starting PbO Powder, Pelletized PbO, and Heat-Treated Pellet (at 500 °C in Ar for 1 h)

Sample	Phase Composition Determined by Rietveld Analysis (Wt Pct)	
	α-PbO (Tetragonal)	β-PbO (Orthorhombic)
Starting PbO Powder	11 pct	89 pct
Pelletized PbO	36 pct	64 pct
Heat-Treated PbO (Ar, 500 °C, 1 h)	0.8 pct	99.2 pct

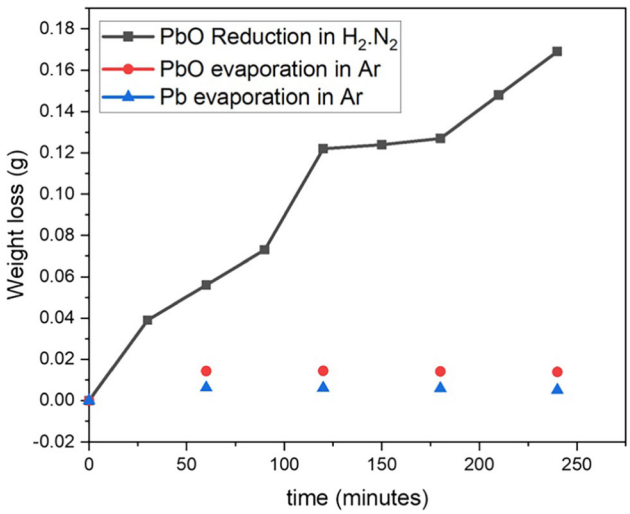

Fig. 4—PbO and Pb evaporations relative to the wright change during PbO reduction under 15 pct H_2-N_2 atmosphere at 700 °C.

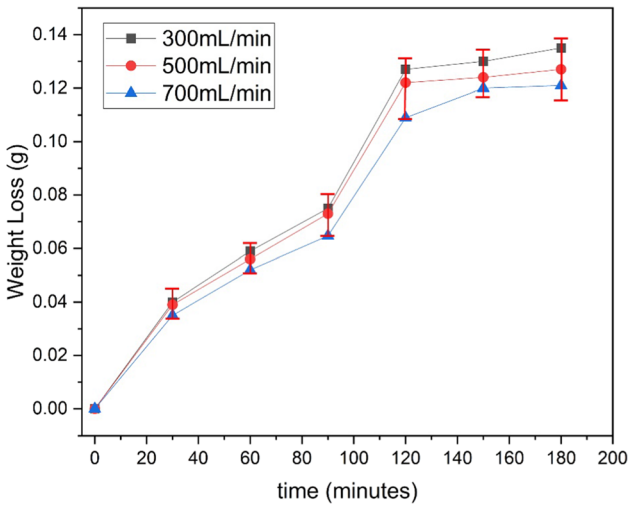

Fig. 5—The effect of gas flowrate on the weight loss/reduction rate of PbO at 700 °C under 15 pct H_2-N_2 gas atmosphere.

bigger droplets among the smaller droplets (Figures 8(a) through (d)) at 600 °C. The same trend was observed for samples reduced at 700 °C; however, the rate of coalescence was observed to be higher compared to those at 600 °C (in line with the overall rate of reduction). However, the variation in the lead droplet size in samples reduced at 700 °C was higher compared to those reduced at 600 °C (Figures 8(e) through (h)). Overall, the lead droplets had size of 0.5 μm in the early time of reduction and could grow up to 500 μm at longer reduction time (at 4 h) for samples reduced at 600 °C. While in samples reduced at 700 °C, the lead droplet size could grow up to 1.5 mm, at 4 h of reduction time (Figure 8h).

Figures 8(e) through (h) also show that upon coalescence of droplets to form bigger ones, a fresh surface of PbO was exposed (please see the arrows indicating the regions). This allowed the H_2 gas to reach and react with the PbO surface; and once that happened, immediate formation of new nano-size (less than 1 μm) Pb droplets on the exposed area was observed. So, it appeared that these continual droplet's coalescence (and removal of these droplets through dripping) is vital for the overall kinetics of the reduction. This will be discussed further in the following section on kinetics and mechanism.

The rate of droplet's coalescence (from SEM observation of the surface) was found to increase with increasing temperature from 600 °C to 800 °C. With more bigger droplets formed at longer reduction time, the chance and hence the frequency of lead dripping to the crucible underneath were also high. These led to the ability of the H_2 to keep reducing the PbO; hence, the overall kinetics were also faster as the temperature was increased from 600 °C to 800 °C. Figure 9 shows the secondary electron images of the surface of the samples reduced at 800 °C. Figures 9(a), (b) and (c) show the surface of the pellet where full coverage of lead had already occurred. Figure 9d and e shows the other areas on the pellet surface where a complete coverage of the surface was yet to occur. At 3 h, all of the PbO had fully reduced and the surface of the lead is shown in Figure 9d.

The observation of numerous lead droplets on the surface of the PbO surface re-emphasizes the fact that the lead is quite non-wetting on the PbO. This is good from the perspective of separation process. High interfacial energy between lead and PbO (indicated by the non-wetting) would ease a clean separation between them. However, it was also clear that the covering of the lead droplets on the flat surface of the PbO hindered the H_2 reductant to reach the PbO to continue the reduction, which has ramification for industrial practice. The detached lead droplets behavior will likely affect the

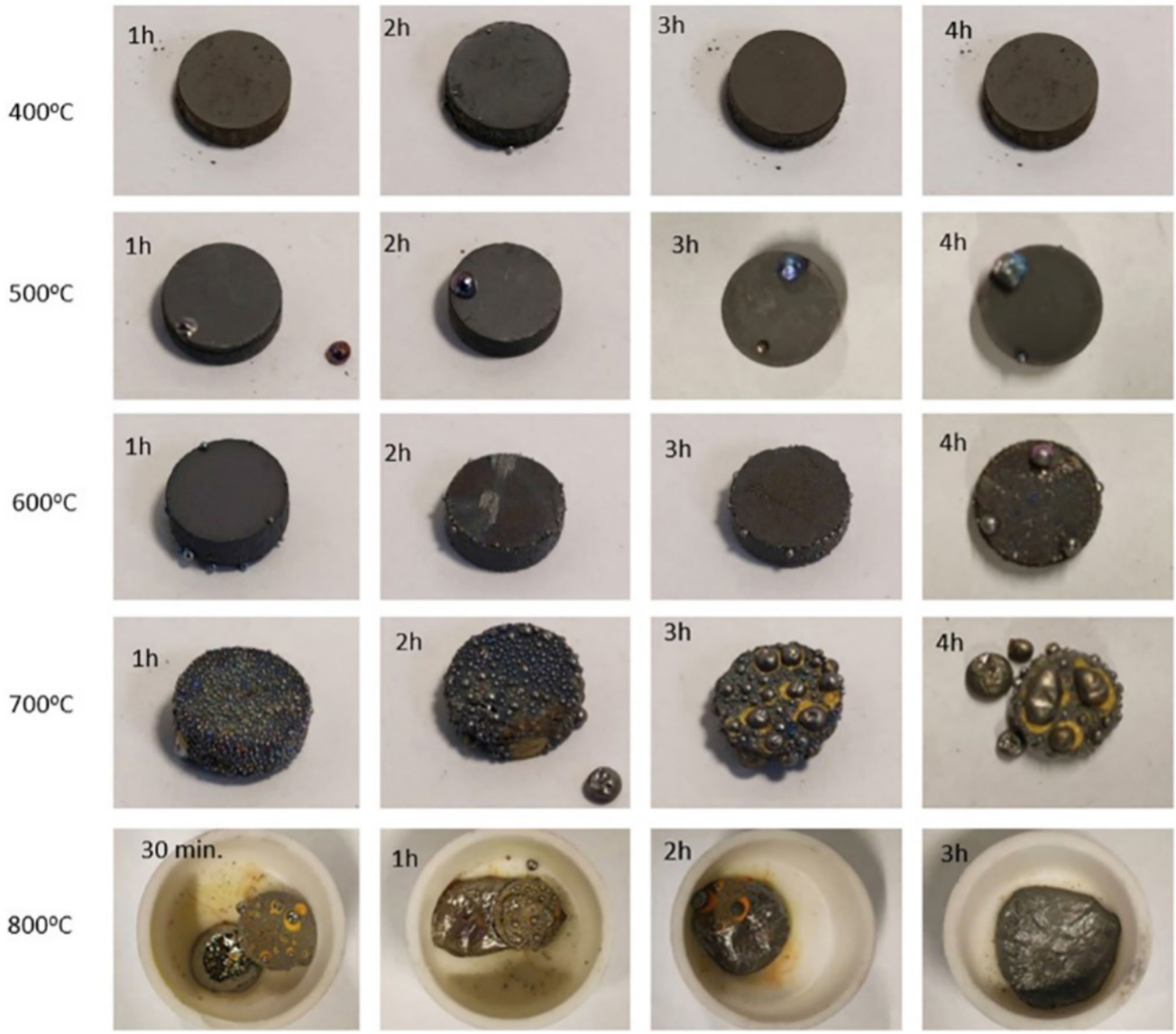

Fig. 6—Macrographs of the PbO pellets' surface after the reduction in 15 pct H_2-N_2 at temperatures 400 °C to 800 °C; and reaction time from 30 min to 4 h.

efficient gas flow in a typical lead blast furnace and might lead to an uneven charge descent.[18,19] In industrial practice, therefore, it is important to ensure that the formed lead droplets are able to easily drain to allow the reduction to continue to completion. Hence, a strategy for the arrangement of how the input charge is distributed in the reactor (such as in blast furnace) will need to be carefully considered. There have been some previous studies that look at methods for improving mode of charging of materials and their distribution, and various modification of air blast injection *via* tuyeres for operation efficiency of blast furnace.[20,21] However, these have focused on operation using coke as reductant and fuel. Having hydrogen as reductant and fuel will provide additional challenges for blast furnace operation. To the author's knowledge, no works in open literatures exist on the use of high concentration of hydrogen for lead blast furnace, although there have been some works in the context of hydrogen in iron blast furnace.[22–26] Therefore, these areas are worthy of further research to facilitate the integration of hydrogen in lead blast furnace.

D. *XRD Phase Analysis*

Two types of XRD phase analyses were carried out, namely powdered and surface analyses. The powdered method involved crushing the reduced pellet into fine powder. The main advantage of this method is that one can get an overall information of phases that exist within the pellet (include those on the surface and at the core). Even though surface visual observation showed a distinguishable color change (Figure 6), cross-section observation revealed unreduced PbO at the core of the pellet, as shown in Figure 10. This unreduced section of the pellet (yellowish phases) was

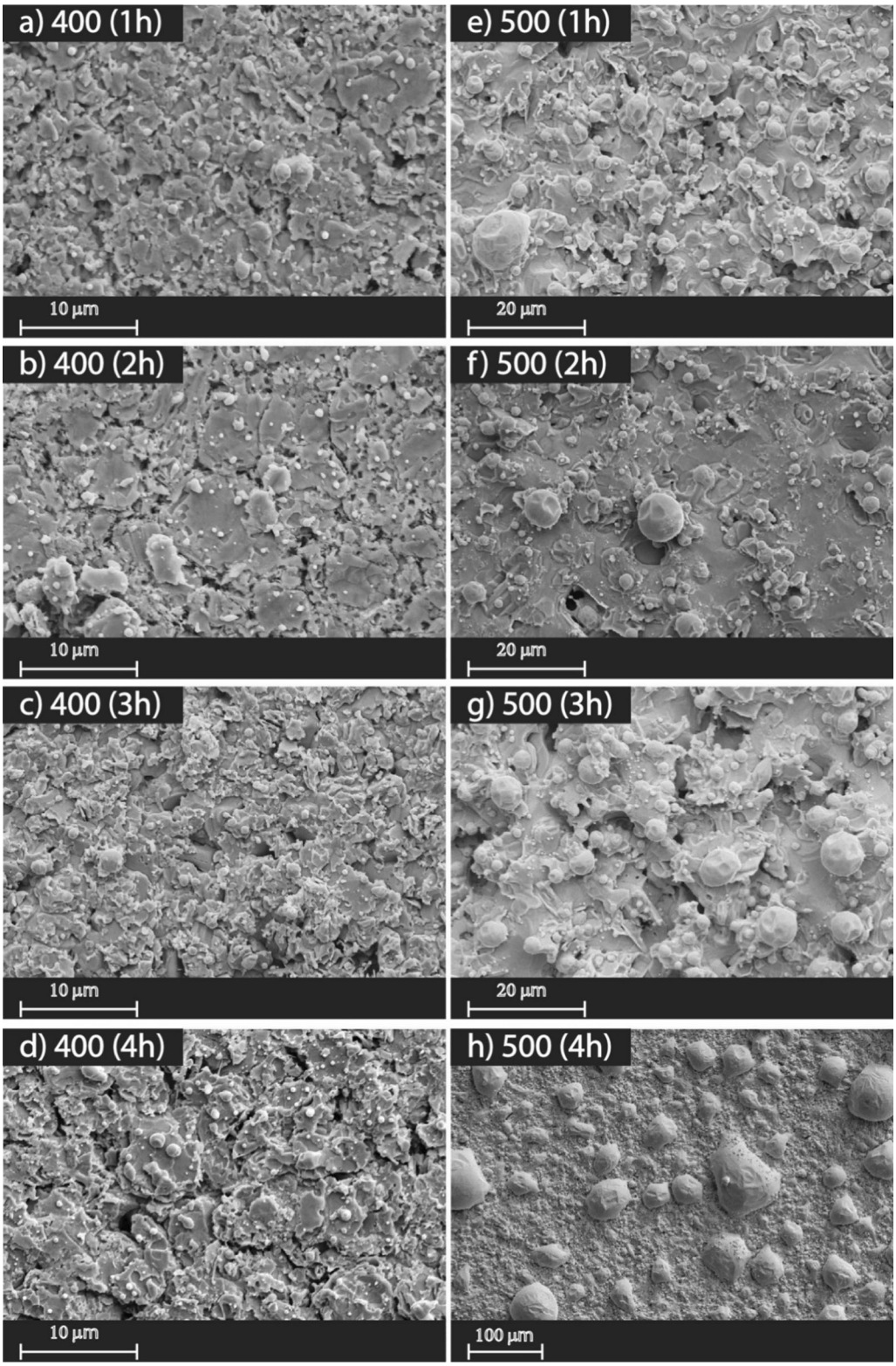

Fig. 7—Secondary electron images of the PbO pellets' surface reduced in 15 pct H_2-N_2 gas at (*a*) 400 °C 1 h; (*b*) 400 °C 2 h; (*c*) 400 °C 3 h; (*d*) 400 °C 4 h; (*e*) 500 °C 1 h; (*f*) 500 °C 2 h; (*g*) 500 °C 3 h; (*h*) 500 °C 4 h.

important to be identified for overall reduction mechanism analysis. However, as the study involved the use of metastable orthorhombic β-PbO phase that was sensitive to stress-induced phase transformation,[14–16] crushing the samples would provide an invalid phase identification and quantification. Therefore, in

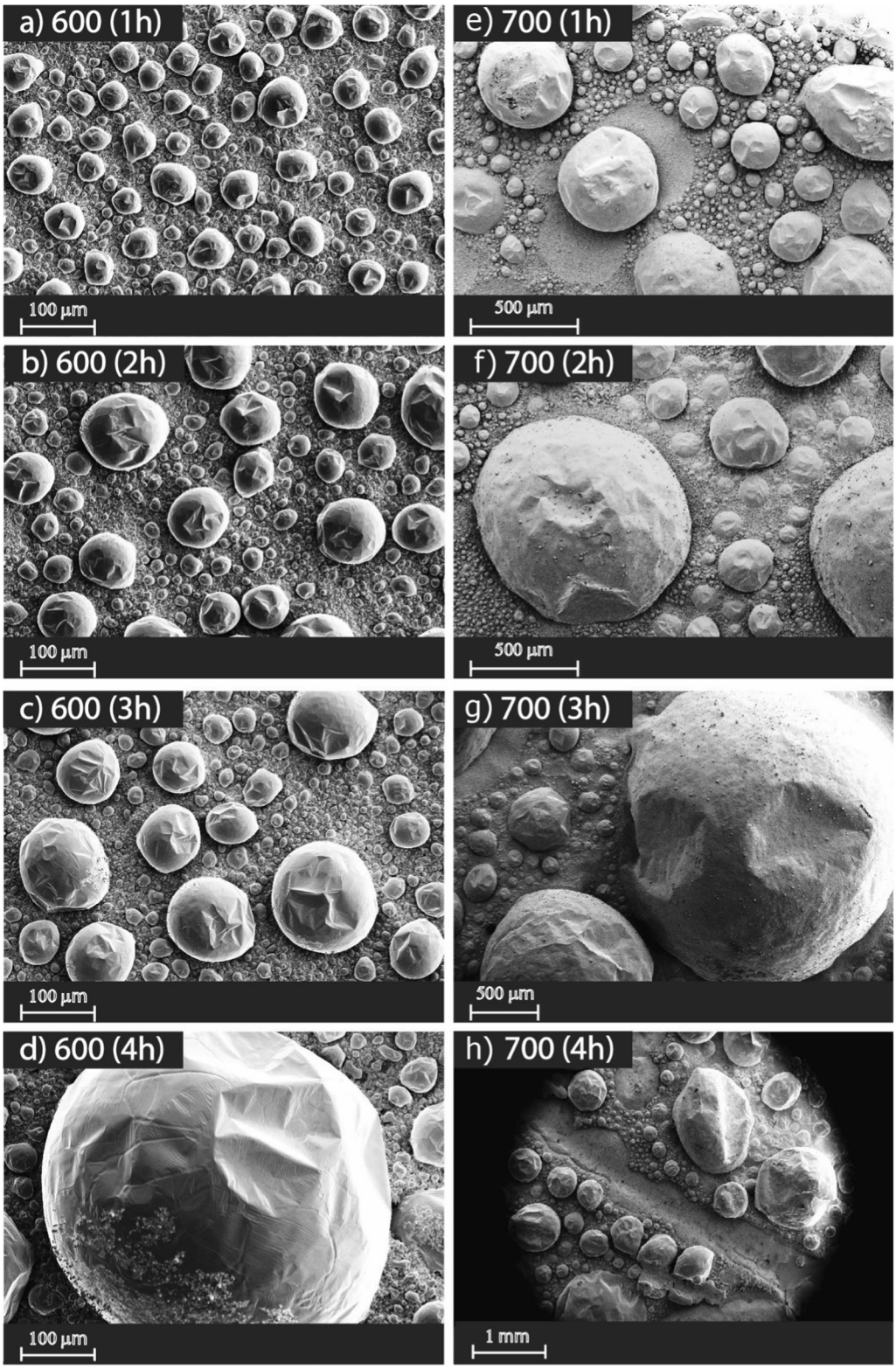

Fig. 8—Secondary electron images of the PbO pellets' surface reduced in 15 pct H_2-N_2 gas at (*a*) 600 °C 1 h; (*b*) 600 °C 2 h; (*c*) 600 °C 3 h; (*d*) 600 °C 4 h; (*e*) 700 °C 1 h; (*f*) 700 °C 2 h; (*g*) 700 °C 3 h; (*h*) 700 °C 4 h.

addition to the powdered samples analyses, surface XRD analyses were also carried out on selected samples to obtain phases information close to the surface.

Figure 11 shows surface XRD analysis results of selected pellet samples after reduction at 400 °C to 700 °C for 4 h. Based on Rietveld quantification, the amount of α-PbO in the sample reduced at 400 °C for

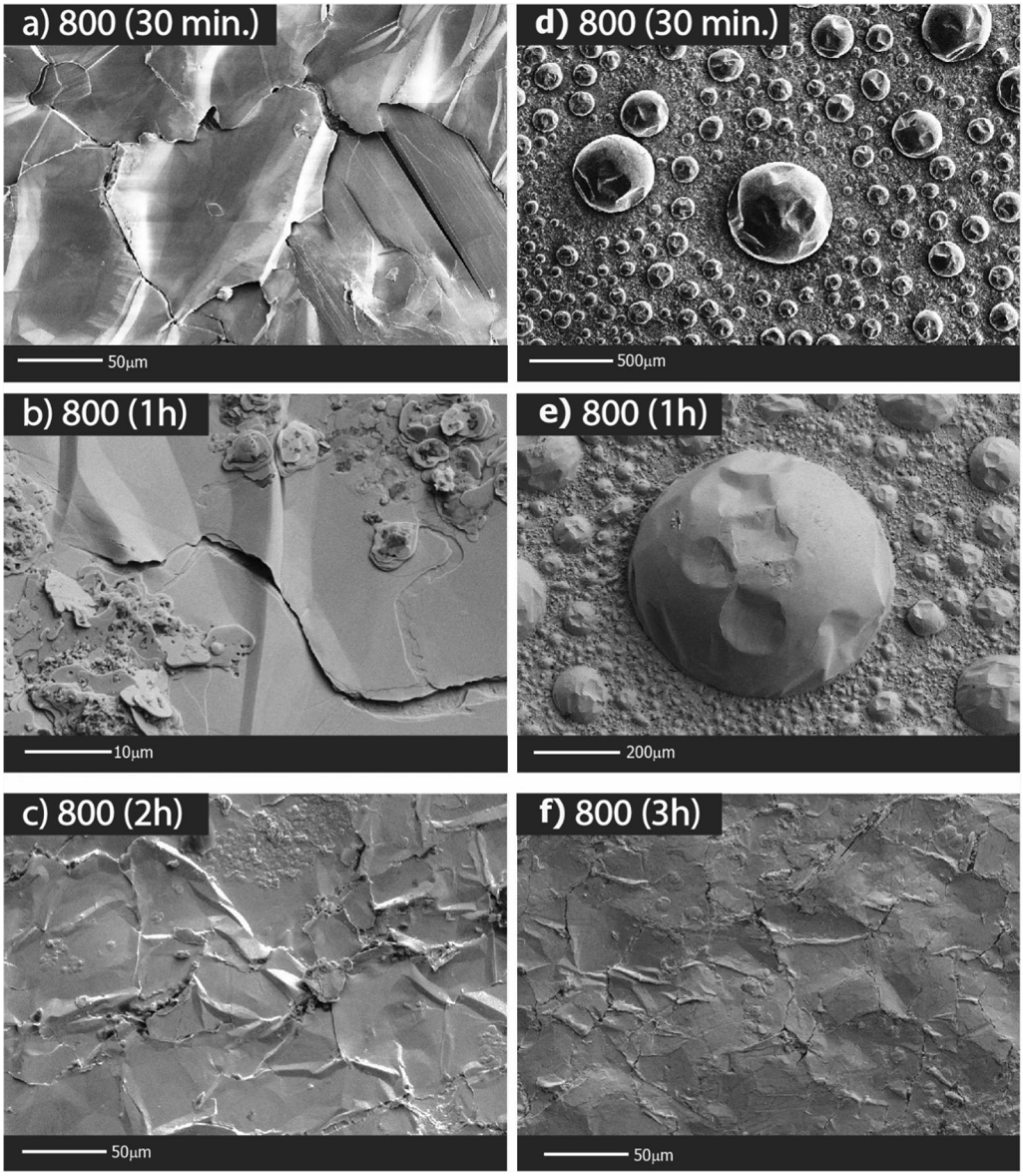

Fig. 9—Secondary electron images of the PbO pellets' surface reduced in 15 pct H_2-N_2 gas at 800 °C, (*a*) at 30 min, showing a layer of lead product; (*b*) at 1 h; (*c*) at 2 h; (*d*) at 30 min and (*e*) at 1 h showing other areas where complete coverage was not yet happened; (*f*) at 3 h where all the PbO has fully reduced to Pb.

4 h was relatively similar to the original pellet sample, as shown in Table III. Lead was also detected at this condition. There were significant α-PbO to β-PbO phase transformations observed from samples reduced at 500 °C and above. This result is in agreement with previous studies that reported the PbO polymorphic transformation at about 500 °C. Meanwhile, the amount of lead on the surface was observed to increase with increasing temperature up to 600 °C. At 600 °C, the amount of lead on the surface was approximately 75 pct. This was in line with the overall SEM observation that shows a high coverage of lead droplets on the pellet surface. However, a lower amount of lead (~ 10 pct) was observed on the surface of pellet sample reduced at 700 °C. This was due to the rapid coalescence of lead droplets on the surface (followed by dripping of the droplets to the crucible) exposing fresh PbO surface during reduction at high temperatures.

The XRD analysis results of powdered pellet samples reduced at 400 °C and 500 °C are shown in Figure 12 along with the Rietveld phases quantification in Table IV (for samples reduced at 400 °C to 700 °C). Tetragonal α-PbO, orthorhombic β-PbO, and also lead peaks were detected on the samples reduced at 400 °C treated for 1 h, 2 h, and 3 h (Figure 12-left). The amount of lead was observed to increase with increasing reduction time, and at the same time, the orthorhombic β-PbO was also decreasing. The samples reduced at 400 °C were transformed into 'gray PbO,' as evidenced by the macrograph Figure 6 and cross section in

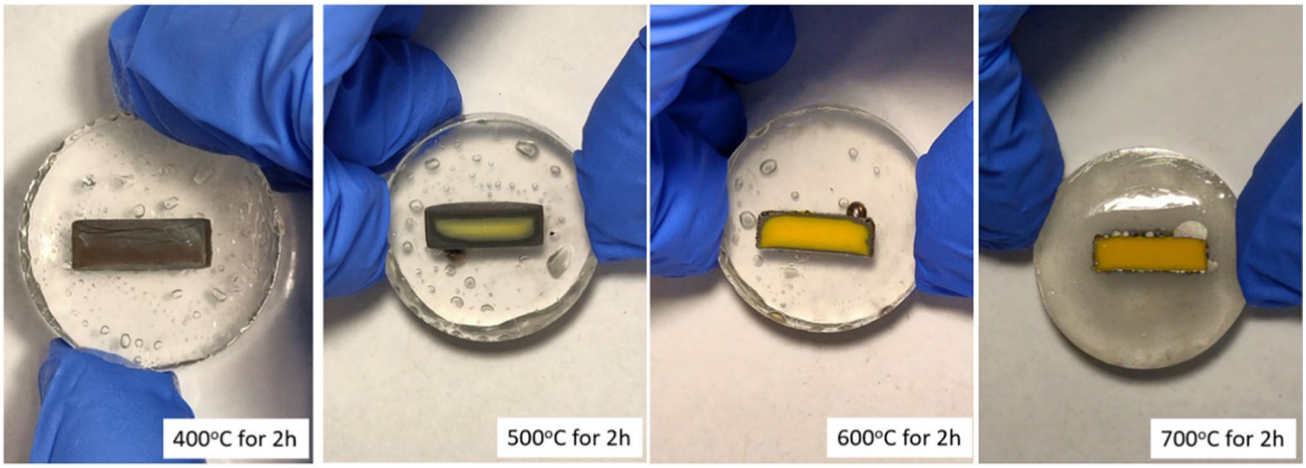

Fig. 10—Cross-section observation of the PbO pellets reduced at 400 °C, 500 °C, 600 °C, and 700 °C for 2 h.

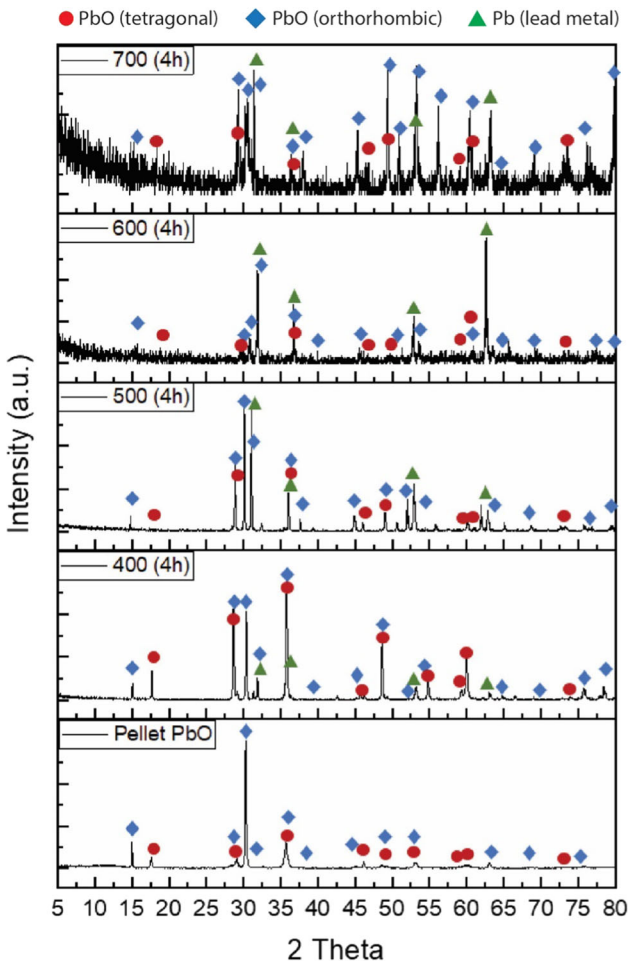

Fig. 11—Surface XRD analysis and Rietveld quantification of original PbO and pellet samples reduced at 400 °C, 500 °C, 600 °C, and 700 °C for 4 h.

Figure 10. The gray PbO or gray oxide (or sometimes called leady oxide) is a mixture of α-PbO and Pb with ratio varies but normally with higher proportion of α-PbO. As the reduction progressed with time, the tetragonal α-PbO dominated the structure of 'gray PbO' as shown in the Rietveld quantification (Table IV), increasing from 57 to 73 pct at 1 h to 3 h reduction, respectively. This, overall, resulted in a less dense pellet (as the density of α-PbO is smaller than β-PbO). The less dense pellet, combined with generation of Pb droplets at nano-size, allowed hydrogen to went through to the center of pellet for further reduction.

The XRD spectra of samples reduced at 500 °C are shown in Figure 12-right. The Rietveld quantification analysis of the samples (Table IV) showed a high amount of β-PbO, which was due to α-PbO → β-PbO phase transformation that happened at temperature at about 500 °C. However, compared to the samples reduced at 400 °C, the samples reduced at 500 °C showed a decreasing amount of lead due to a diffusion-controlled process (will be explained in the kinetics Section III–E). The evidence of diffusion-controlled process was reflected on the cross section shown in Figure 10. Samples reduced at 500 °C and above went through a phase transformation in the whole pellet body and at the same time faster oxide reduction on the surface. Faster reduction was resulting in high lead formation covering on the surface. In samples reduced at temperatures between 500 °C and 600 °C, in particular, no Pb dripping was observed. This resulted in the accumulation of Pb and formation of a Pb layer on the surface which provide an obstacle for hydrogen diffusion to the samples' interior. This was also supported by the increase of lead intensity on surface XRD analyses of the samples reduced at 500 °C compared to those reduced at 400 °C (an increase by about 20 pct), as shown in Table III.

PbO reduction by hydrogen on the surface of the samples reduced at 600 °C occurred even more rapid which consequently created a similar lead layer that covered the surface. This lead layer can also be seen on the cross-sectioned sample (Figure 10) and also reflected on the surface XRD analysis result (Table III). However, the XRD analysis of the powdered samples reduced 600 °C in Figure 13-(left) hardly showed any lead. This happened presumably due to unevenly

Table III. Rietveld Refinement Phase Quantification Results of Surface XRD Analyses of Original PbO Pellet and Reduced Pellets at 4 h at 400 °C to 500 °C

Sample		Phase Composition Determined by Rietveld Analysis (Wt Pct)		
Temperature (°C)	Reduction Time (h)	α-PbO (Tetragonal)	β-PbO (Orthorhombic)	Pb (Cubic close-packed)
PbO Pellet	—	36	64	—
400	4	31.5	65.5	4
500	4	2	76.5	21.5
600	4	—	25	75
700	4	—	90	10

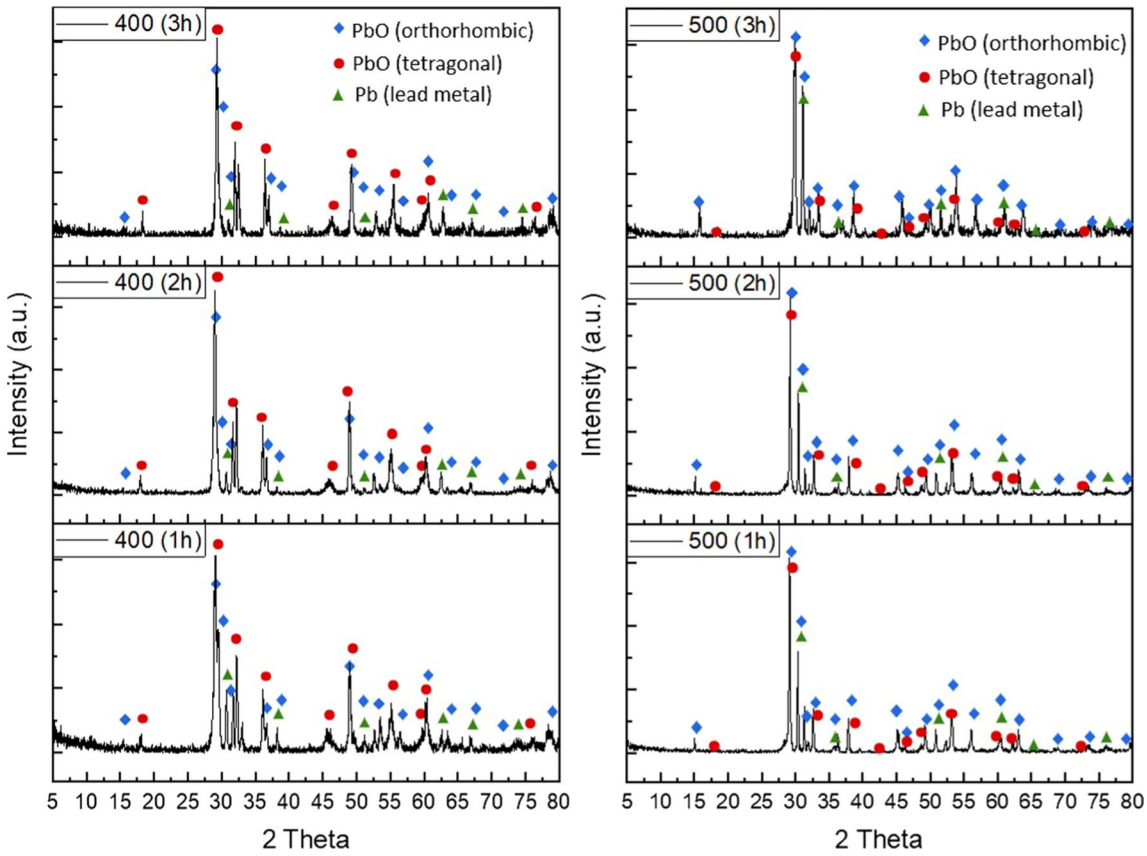

Fig. 12—Powdered XRD analysis and Rietveld quantification of pellet samples reduced at 400 °C (left) and 500 °C (right) for 1 to 3 h.

dispersed of lead within the crushed powder. It should also be noted that at 600 °C, coalescence of the droplets on the surface was already observed (Figure 8).

Surface XRD analyses were applied for samples reduced at 700 °C due to difficulty of grinding the lead droplets down into fine powder. The XRD results are shown in Figure 13-(right), which revealed a high amount of orthorhombic β-PbO and Pb with small amount of α-PbO. Theoretically, the α-PbO should had been converted into β-PbO at temperature above polymorphic transition. The detection of small amount of α-PbO was presumably due to the mechanical force during sample crushing which caused some β-PbO converted back into α-PbO.

It is worth noting that from the macrograph, morphology, and phase observations, one can observe a phase transformation of PbO phase from tetragonal-(α) to orthorhombic-(β) due to heating above its polymorphic transition temperature. This transformation will be included the analysis of micromechanism (in the subsequent Subsections) as one was able to observe a gray PbO formation which contains a mixture of one of PbO phase with Pb. However, these phase transformations appeared to not affect the overall kinetics, which also has been reported in the previous study by Ivanov *et al.*.[7]

Table IV. Rietveld Refinement Phase Quantification Results of XRD Analysis of Powdered Samples Reduced at 400 °C to 700 °C for 1 to 3 h

Sample		Phase Composition Determined by Rietveld Analysis (wt pct)		
Temperature (°C)	Reduction Time (h)	α-PbO (Tetragonal)	β-PbO (Orthorhombic)	Pb (Cubic close-packed)
400	1	57.6	36	6.3
	2	73.8	15.4	10.8
	3	73.2	11.5	15.3
500	1	9.5	85.7	4.8
	2	8	87.3	4.7
	3	7	87	6
600	1	7	93	—
	2	6.7	92.6	0.7
	3	6	92	2
700*	1	—	75.8	24.2
	2	1.3	81.7	17
	3	5.2	81.2	13.6

*surface XRD analyses.

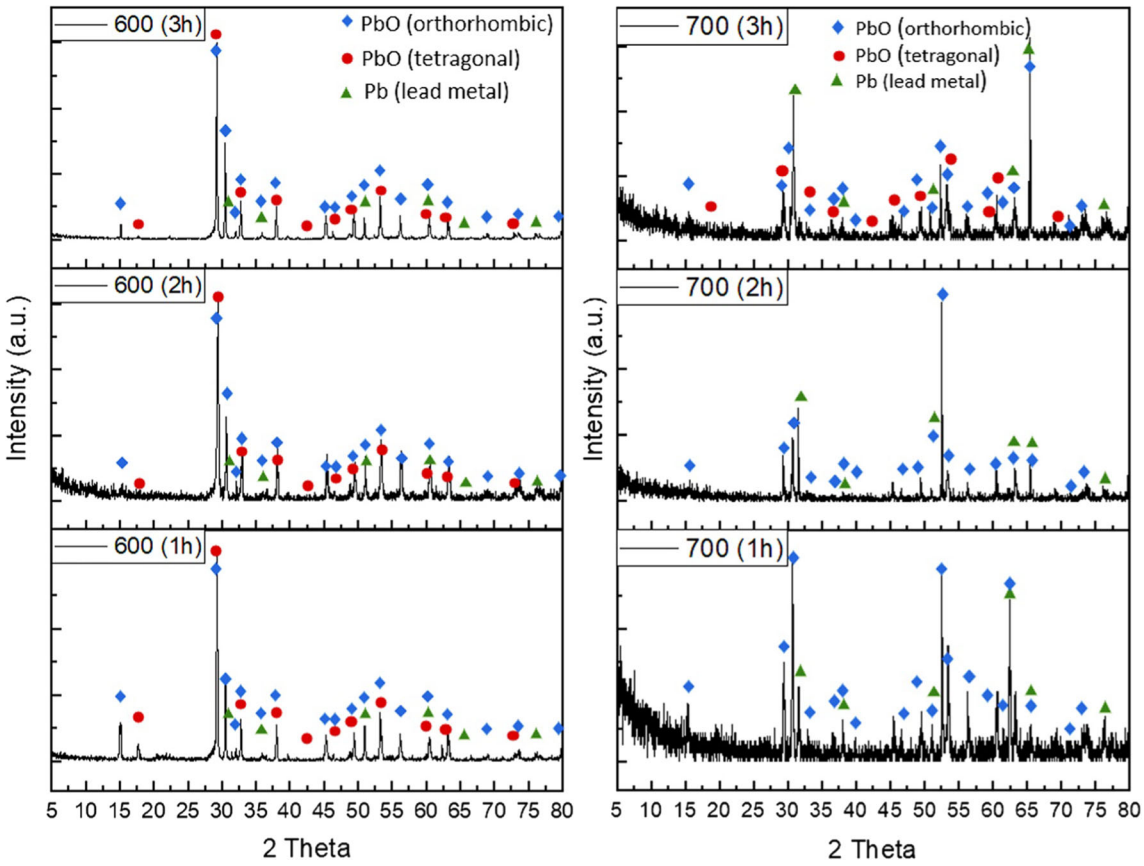

Fig. 13—XRD analysis and Rietveld quantification of powdered pellet samples reduced at 600 °C (left) and surface of pellet samples reduced at 700 °C (right) for 1 to 3 h.

E. *Kinetics Analyses of PbO Reduction by Hydrogen*

The samples' weight measured after the reduction experiments were converted into extent/degree of reduction (α) according to Eq. [1], and the results are presented as a function of time in Figure 14. In general, the reduction degree was observed to increase with increasing reduction time. However, the variation of the reduction degree with increasing temperature was not straight forward. The reduction degree (at 2 h of reduction) was first observed to increase with increasing temperature from 350 °C to 475 °C, *i.e.*, from 10 to 30 pct, respectively. From 500 °C to 600 °C, the reduction

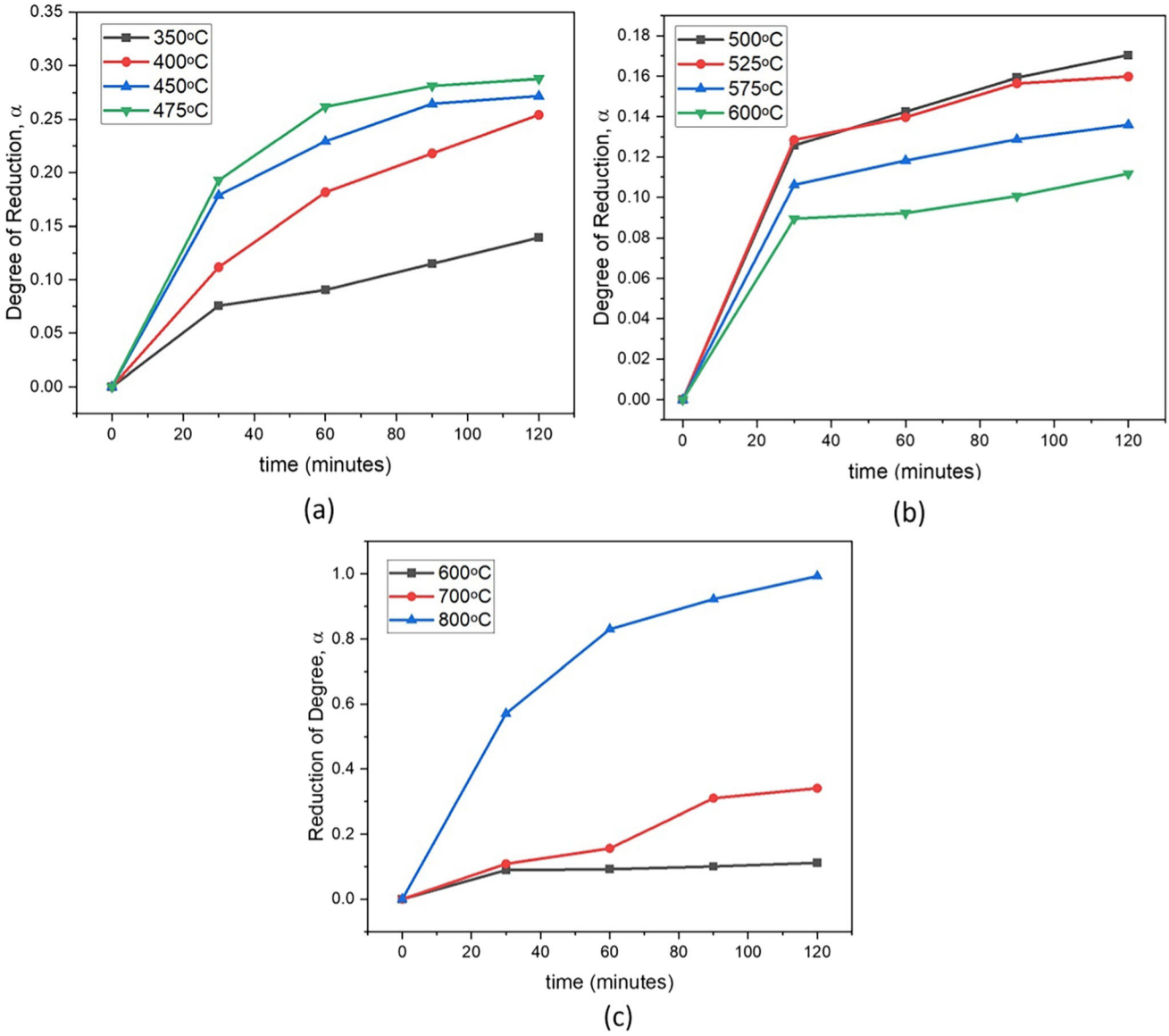

Fig. 14—Degree of reduction as a function of time of the PbO pellet samples reduced in 15 pct H_2-N_2 atmosphere at temperatures (*a*) 350 °C to 475 °C; (*b*) 500 °C to 600 °C; and (*c*) 600 °C to 800 °C.

degree was observed to decrease from only 15 pct to under 10 pct, before increased steeply above 600 °C. A sharp increase of reduction degree was observed at 800 °C and it reached a complete reduction after 120 minutes.

The reduction degree behavior with respect of temperature can be explained by looking at the samples' cross section along with the macrograph observations and the XRD analysis results, and this has been briefly discussed in Section III–C. At 350 °C to 475 °C, the cross-section observation showed that the reduction appeared to occur into the interior of PbO pellet where fine nano-size Pb nuclei (less than 1 μm) were formed but large micro-droplets were not formed yet. The mixture of fine Pb and unreduced PbO that formed a 'gray PbO' appeared to be relatively less dense (maintained its open connected pores) which allowed hydrogen to diffuse to the center of the pellet, which consequently, more PbO (both α and β-PbO) were reduced. This was supported by the XRD results of powdered samples shown in Figure 12 as well in Table IV. Therefore, in the temperature range of 350 °C to 475 °C, the reduction could progress and the reduction degree increased with increasing temperature.

Between 500 °C and 600 °C, the initial formation of the fine lead droplets was quite fast and quickly covered the surface. With further reduction time, some of the lead droplets coalesce; however, the rate of lead droplets coalescence and droplets dripping was not that high; hence, the lead was accumulated on the surface. This resulted in a thicker lead layer with increasing

Table V. Calculated k (Constant Rate) and R^2 (Regression Linier Coefficient) from Fitting of Various Kinetic Models for the Reduction of PbO Pellets at 350 °C to 800 °C

	350 °C		400 °C		450 °C		475 °C		500 °C	
Kinetics Model (Conversion Factor)	k	R^2	k	R^2	k	R^2	k	R^2	k	R^2
Order of Reaction										
F1	0.0014	0.9662	0.0027	0.9809	0.0033	0.9200	0.0036	0.9374	0.0017	0.9078
F2	0.0126	0.8530	0.0142	0.8775	0.0150	0.8619	0.0154	0.8700	0.0130	0.8486
F3	0.0142	0.8716	0.0182	0.9148	0.0202	0.8660	0.0213	0.9015	0.0152	0.8597
Nucleation and Growth										
A2 $(-\ln(1-\alpha)^{1/2})$	0.0007	0.9662	0.0013	0.9809	0.0017	0.9200	0.0018	0.9374	0.0009	0.9078
A3 $(-\ln(1-\alpha)^{1/3})$	0.0005	0.9560	0.0010	0.9842	0.0011	0.9200	0.0012	0.9374	0.0006	0.9078
A4 $(-\ln(1-\alpha)^{1/4})$	0.0003	0.9662	0.0007	0.9809	0.0008	0.9200	0.0009	0.9374	0.0004	0.9078
Geometry Models										
R1 (α)	0.0013	0.9618	0.0024	0.9738	0.0029	0.9127	0.0031	0.9269	0.0016	0.9031
R2 $(1-(1-\alpha)^{1/2})$	0.0007	0.9640	0.0013	0.9774	0.0015	0.9163	0.0017	0.9322	0.0008	0.9054
R3 $(1-(1-\alpha)^{1/3})$	0.0004	0.9647	0.0009	0.9786	0.0011	0.9175	0.0011	0.9339	0.0006	0.9062
Diffusion Models										
D1 $(\alpha 2)$	0.00020	0.9944	0.0005	0.9982	0.0007	0.9490	0.0009	0.9747	0.0002	0.9420
D2 $(\alpha + (1-\alpha)\ln(1-\alpha))$	0.00008	0.9940	0.0003	0.9976	0.0004	0.9530	0.0005	0.9776	0.0001	0.943
D3 $((1-(1-\alpha)^{1/3})^2)$	0.00002	0.9935	0.00007	0.9966	0.0001	0.9529	0.0001	0.9803	0.00003	0.9439
D4 $(1-2\alpha/3-(1-\alpha)^{2/3})$	0.00002	0.9938	0.00007	0.9973	0.00009	0.9517	0.00001	0.9785	0.00003	0.9433

	525 °C		575 °C		600 °C		700 °C		800 °C	
Kinetics Model (Conversion Factor)	k	R^2	k	R^2	k	R^2	k	R^2	k	R^2
Order of Reaction										
F1	0.0019	0.8819	0.0015	0.8991	0.0012	0.8943	0.0036	0.9869	0.0356	0.9678
F2	0.0132	0.8422	0.0127	0.8427	0.0124	0.8403	0.0155	0.9126	0.7215	0.6259
F3	0.0156	0.8506	0.0146	0.8519	0.0138	0.8471	0.0218	0.9627	99.527	0.5402
Nucleation and Growth										
A2 $(-\ln(1-\alpha)^{1/2})$	0.0009	0.8819	0.0008	0.8991	0.0006	0.8945	0.0018	0.9869	0.0178	0.9678
A3 $(-\ln(1-\alpha)^{1/3})$	0.0006	0.8819	0.0005	0.8991	0.0004	0.8943	0.0012	0.9869	0.119	0.9678
A4 $(-\ln(1-\alpha)^{1/4})$	0.0005	0.8819	0.0004	0.8991	0.0003	0.8945	0.0009	0.9869	0.089	0.9678
Geometry Models										
R1 (α)	0.0017	0.8789	0.0014	0.8955	0.0011	0.8914	0.0030	0.9884	0.0100	0.9406
R2 $(1-(1-\alpha)^{1/2})$	0.0009	0.8804	0.0007	0.8973	0.0006	0.8928	0.0016	0.9881	0.0082	0.9872
R3 $(1-(1-\alpha)^{1/3})$	0.0006	0.8809	0.0005	0.8979	0.0004	0.8933	0.0011	0.9878	0.0068	0.9963
Diffusion Models										
D1 $(\alpha 2)$	0.0003	0.9084	0.0002	0.9424	0.0001	0.9340	0.0009	0.9405	0.0091	0.9864
D2 $(\alpha + (1-\alpha)\ln(1-\alpha))$	0.0001	0.9096	0.00009	0.9441	0.00006	0.9383	0.0005	0.9352	0.0081	0.9982
D3 $((1-(1-\alpha)^{1/3})^2)$	0.00003	0.9108	0.00002	0.9459	0.00001	0.9397	0.0001	0.9296	0.0045	0.9479
D4 $(1-2\alpha/3-(1-\alpha)^{2/3})$	0.00003	0.9100	0.00002	0.9447	0.00001	0.9388	0.0001	0.9333	0.0024	0.9945

temperature and time and provided a bigger barrier. Hence, the reduction degree decreased with increasing temperature. Similarly, at temperatures between 600 °C and 800 °C, the initial lead droplets were formed quickly and abundantly on the surface of the samples. However, the rate of droplets coalescence and droplets dripping was significantly higher compared to those at 500 °C to 600 °C. The higher temperatures meant that the surface tension and viscosity of the lead were also lowered[27,28] which further facilitated the lead dripping and draining from the samples. This resulted in a continual formation of fresh PbO surface, which allowed the reduction to proceed faster with increasing temperature.

The discussion presented in the previous revealed that the reduction process was very likely to be controlled by diffusion, as evidenced by SEM analyses of the samples surface, macro- and cross-section observations, as well as preliminary experiments on the effect of gas flowrate (Section III–C). With this in mind, further kinetics analyses were carried out by evaluating different kinetic models that associated with nucleation, grain growth, and difussion. These included the calculation of rate parameter (as a function α), the k (constant rate), and R^2 value from the different models, in which the results are summarized in Table V. It can be seen that the reduction can be reasonably fitted into Jander (D3) and Ginstling-Brounhstein (D4) diffusion models. The R^2 values of the D3 and D4 diffusions model are in the range of 91 pct to 99 pct. It should be noted that previous study of PbO reduction by hydrogen reported to the process to controlled by first-order reaction (A1)[5] and inter-particle diffusion (D3) in the case of reduction using a bed of PbO particles.[3]

Jander model uses a parabolic law, Eq. [2], as a basic formulation to describe a continuously decreasing extent of reaction over time progression. In the case of a 3D sphere particle, the equation can then be presented as Eq. [3]. Jander 3D model can also be applied for other

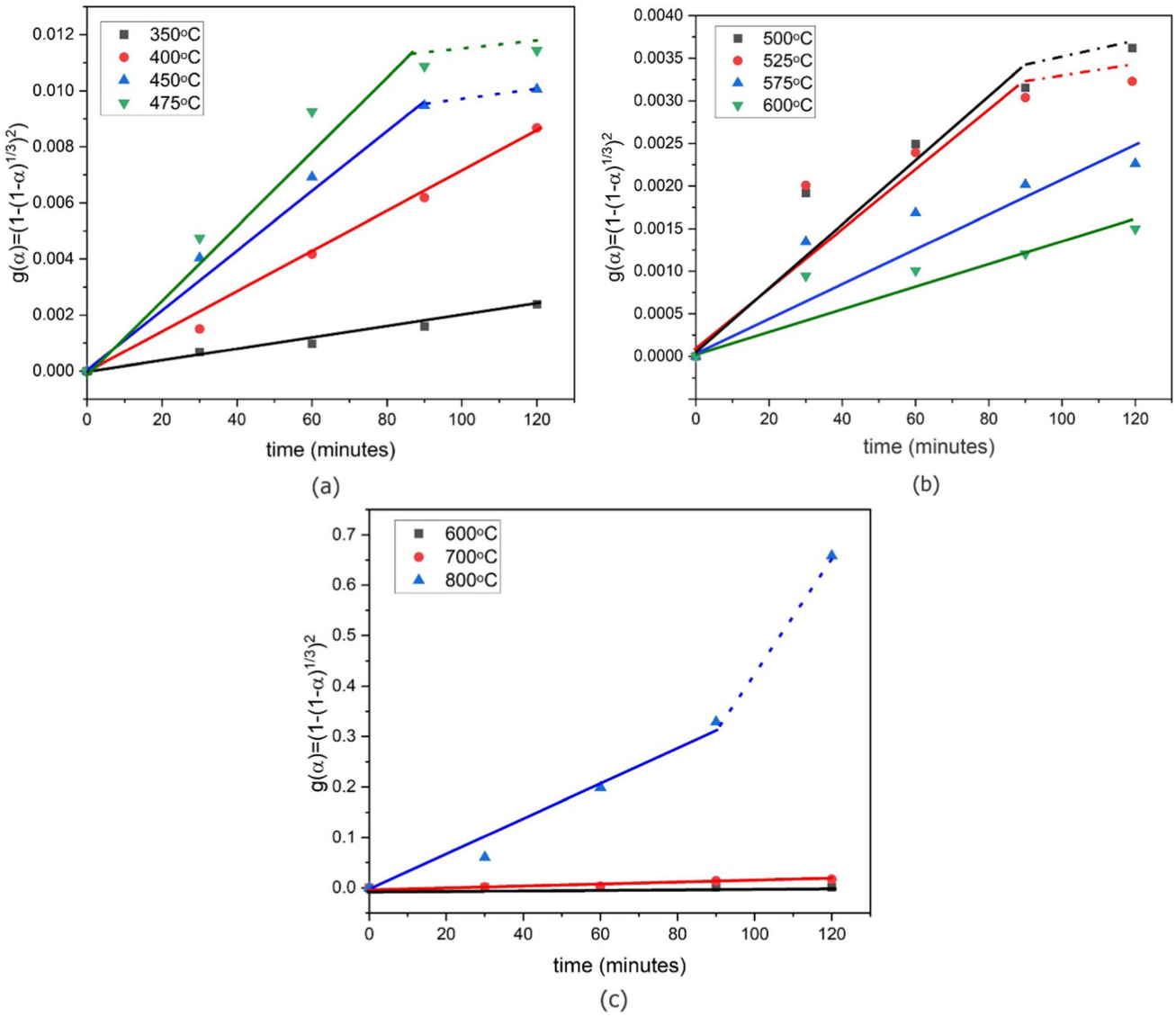

Fig. 15—Plots of kinetics data using Jander model for samples reduced at: (*a*) 350 °C to 475 °C, (*b*) 500 °C to 600 °C, and (*c*) 600 °C to 800 °C.

shapes such as pressed or compacted powder (pellet), where the sphere is considered to have *n* number of particles.[29] Jander model assumes no change in solid volume and density during reaction. Consequently, the model is accurate for low reduction degree (extent of reaction).[12] The Ginstling-Brounhstein (GB) model is an improvement of Jander model with a correction to this assumption and presented in Eq. [4].[13] Both Jander and GB models showed similar kinetic graph fitting for the data from the current study with similar R^2 (although the R^2 of the GB was slightly lower compared to Jander). It was noted from the experiments that the shape of the majority of the samples did not experience significant change in size except those reduced at 700 and 800 °C. Therefore, for simplicity, Jander model was used to evaluate the kinetics data of PbO pellets reduction.

$$x = R\left[1 - (1-\alpha)^{\frac{1}{3}}\right] \qquad [2]$$

$$kt = \left[1 - (1-\alpha)^{\frac{1}{3}}\right]^2 \qquad [3]$$

$$kt = 1 - \frac{2\alpha}{3} - (1-\alpha)^2 \qquad [4]$$

$$k = A\exp\left(-\frac{E_a}{RT}\right) \qquad [5]$$

The plots of the kinetics data using the Jander model are presented in Figure 15. It can be seen that the data can be reasonably fitted into a straight line using the model. It should be noted that it is quite likely that the rate-controlling mechanism could change as the reaction proceeds with time. Hence, the kinetics data were considered from the early stage of the reactions, *i.e.*,

some of the plots were fitted by considering the first three to four data points only (full lines in the Figure). The slope of the line represents the rate constant (k). The apparent activation energy of PbO reduction can be obtained by plotting the ln k with $1/T$ following the Arrhenius formula Eq. [5], in which the slope of the line represents the (- E_a/R). The plot is presented in Figure 16.

It can be seen from Figure 16 that there are three distinct temperature ranges from the plot representing three different kinetic regimes, *i.e.*, (I) 350 °C to 475 °C, (II) 500 °C to 600 °C, and (III) 600 °C to 800 °C. In the temperature range of (I) 350 °C to 475 °C and (III) 600 °C to 800 °C, the rate constant was found to increase with increasing temperature, and the apparent activation energy was calculated to be 61 kJ/mol and 224 kJ/mol, respectively. For comparison, the activation energy of PbO reduction in hydrogen atmosphere reported in the previous studies is presented in Table VI. It can be seen that the activation energy for the temperature range (I) was close to that reported by Ricapito *et al.*.[4] Ricapito *et al.* did not proposed any rate-limiting step in their study. From the characterization results and observations of the cross section of the pellets, it is plausible that the reduction process in the temperature range (I) was controlled by the diffusion of the hydrogen through the gray PbO (mixture of PbO with fine Pb).

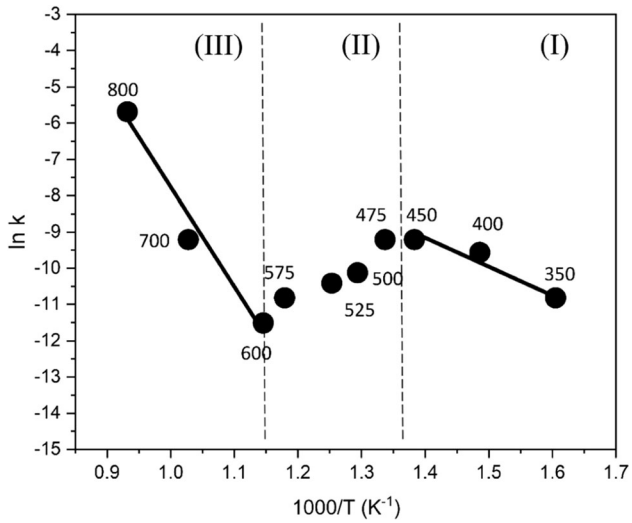

Fig. 16—Arrhenius plot of the rate constants following the Jander model from the experiments.

In the temperature range of (II) 500 °C to 600 °C, the rate constant was found to decrease with increasing temperature. This anomalous variation of k with temperature was due to the phenomenon occurring in this temperature range where thick lead layer was forming and accumulating on the surface, and this range represented a transition from kinetics regimes (I) to (III). Therefore, the k in this temperature range, calculated using the approach in the current study, should be taken as indicative.

In the temperature range of (III) 600 °C to 800 °C, the kinetics were quite fast and the effective energy activation was quite high, *i.e.*, 224 kJ/mol. This energy activation is much higher compared to the previous work of Culver *et al.*[3] in a similar temperature range. The cross-section observation of the pellet samples also revealed a thick Pb layer on the surface. Hence, it was plausible that the reduction process was controlled by hydrogen diffusion through this Pb layer, and the coverage of the Pb layer will significantly affect the kinetics. Overall, the process and the kinetics behavior were quite complex; the Pb layer coverage on the surface would be governed by an overall net effect of the rate of droplets nucleation and coalescence, the rate of formation of fresh PbO surface upon droplets coalescence, and the rate of dripping which would be affected by surface/interface tension and viscosity of the lead and available path for draining.

F. *Overall Reduction Macromechanism*

Considering the results presented in the previous Sections, an overall reduction macromechanism for PbO pellet reduction in 15 pct H_2-N_2 was proposed which consist three major mechanisms, as schematically presented in Figure 17. First, the mechanism for samples reduced at 400 °C or below the polymorphic transformation mainly involves a chemical reduction of PbO and gray PbO formation. This mechanism is in line with kinetics regime (I) 350 °C to 475 °C. At this temperature, there is no polymorphic transition from tetragonal α-PbO to orthorhombic β-PbO as the minimum energy for lattice contraction has not reached. It this temperature range, it appeared that a direct reduction of orthorhombic β-PbO by hydrogen occurred followed by formation of gray PbO (Pb.2PbO). Based on the lattice crystal structure, there is a high probability of

Table VI. Activation Energies (E_a) of PbO Reduction in Hydrogen Atmosphere from Selected Studies

Range of Temperature (°C)	Type of Sample	E_a (kJ/mol)	References
475–775	packed bed of PbO powder	163.18	Culver *et al.* [3]
250–400	PbO in liquid Pb-Bi	67.7	Ricapito *et al.* [4]
450–525	packed bed of PbO powder	85.8 (β-PbO) 93.1 (α-PbO)	Ivanov *et al.* [5]
350–475	pelletized PbO	61	This study
600–800		224	

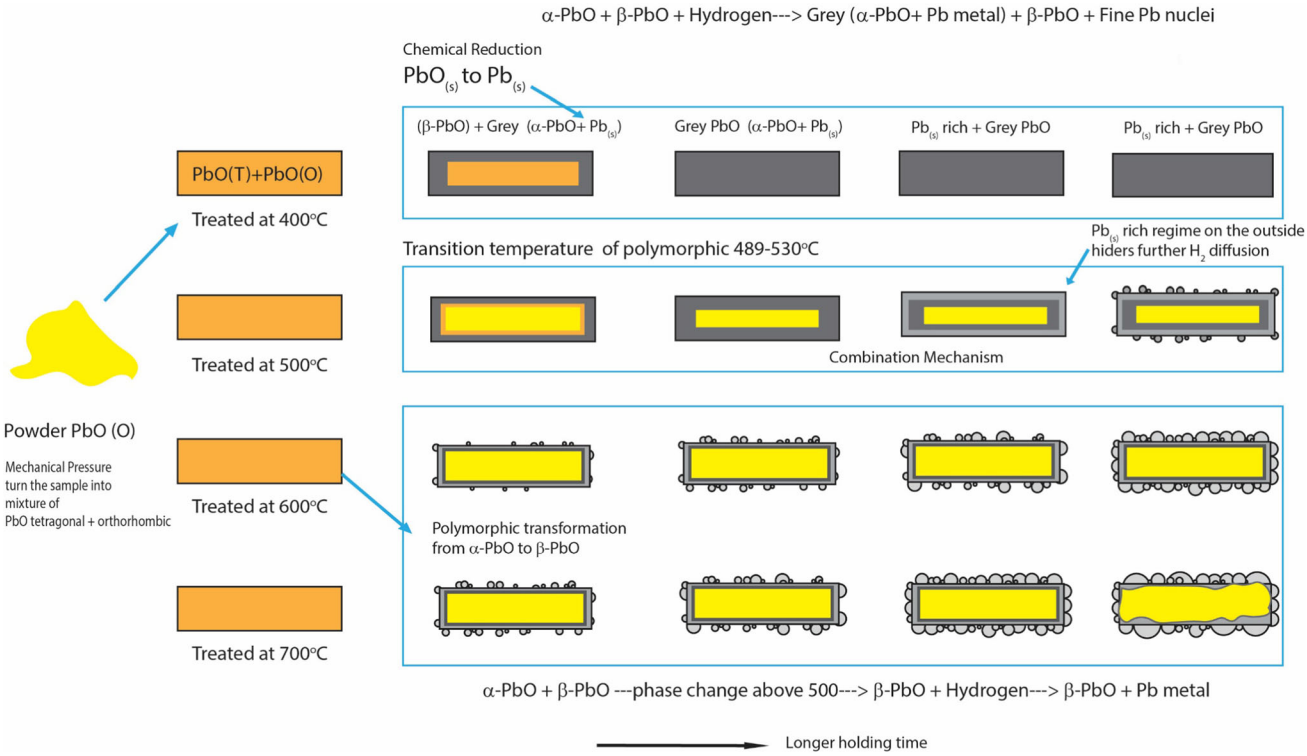

Fig. 17—Proposed overall reduction macromechanism for PbO reduction in 15 pct H_2-N_2 at 400 °C to 800 °C.

orthorhombic β-PbO to be reduced by hydrogen compared to tetragonal α-PbO. Space in the orthorhombic β-PbO is larger than the tetragonal α-PbO by 13 pct along the (100) plane and 18 pct along the (001) plane (Pavlov, 2017). As reflected in the XRD result, the orthorhombic β-PbO was observed to decrease at the same time of increase in Pb. The Pb that was formed by hydrogen reduction then associated with tetragonal α-PbO and the remaining orthorhombic β-PbO in the sample to form 'gray PbO.' The formation of gray PbO is the main reason of color change of the pellet from reddish to gray. This temperature range is beyond the melting point of lead (T_m = 327 °C); however, the formed fine lead was scattered across the sample and had not reach the critical radius for nucleation of large Pb droplets.

The second mechanism is for samples reduced at above the PbO polymorphic transformation temperature. This is in line with the kinetics regime (III) 600 °C to 800 °C. In this temperature range, the pellet samples were first undergoing a phase transformation from tetragonal α-PbO to orthorhombic β-PbO which then followed by reduction to Pb. The pre-existed orthorhombic β-PbO at the same time would also go through reduction by hydrogen to form Pb. In this temperature range, the rate of nucleation, growth, and coalescence of the Pb droplets were very high. However, at the same time, the rate of dripping and draining of Pb from the samples was also high, which was able to continuously create a fresh PbO surface to allow continuous reduction by hydrogen.

The third mechanism is a transition mechanism which combined the two previous mechanisms, mainly occurred in samples reduced around the PbO polymorphic transformation. This is in line with the kinetics regime (II) 500 °C to 600 °C. In this temperature range, the phase transformation from tetragonal α-PbO to orthorhombic β-PbO is occurring, and both gray PbO and significant amount of Pb were also observed to form. The rate of nucleation, growth, and coalescence of the Pb droplets were quite high and enough to provide coverage of the surface. However, this was not matched by the rate of Pb dripping and draining. The resulting accumulated Pb on the surface provides a barrier and hindered further reduction by hydrogen. Therefore, the overall reduction degree in this temperature range was lower compared to those in 350 °C to 475 °C. The gray PbO structure observed the lower temperature range of 350 °C to 475 °C that was more loose and allowed hydrogen to diffuse through the samples' interior which consequently more PbO to be reduced.

IV. CONCLUSION

The current work established a fundamental knowledge on lead reduction from lead monoxide pellets using diluted hydrogen (15 pct H_2-N_2) at 350 °C to 800 °C. A detailed and systematic microstructure evolution during reduction combined with isothermal reduction kinetics analyses was presented. The key findings from the current study are as follows:

- The results from microstructure observation showed that globular and non-wetting lead droplets formed on the surface of PbO samples. It was also observed that this lead droplets layer, once covered the whole surface, appeared to reduce the overall reduction rate. The droplet's diameter was observed to increase with increasing temperature and reduction time.
- The reduction mechanism was found to be complex involving PbO polymorphic phase transformation, PbO reduction to Pb, and diffusion-limited process. In addition to this, the rate of Pb nucleation, rate of Pb droplets coalescence, and rate of Pb dripping and draining play an important role on the overall reduction process.
- A reduction macromechanism consisting three different mechanisms has been proposed which in line with three different kinetics regimes based on temperature range, *i.e.*, (I) 350 °C to 475 °C, (II) 500 °C to 600 °C, and (III) 600 °C to 800 °C. In the temperature range (I), the reduction appeared to be controlled by diffusion in the gray PbO layer, with apparent energy activation of 61 kJ/mol; while in the temperature range (III), the reduction appeared to be controlled by diffusion in thick Pb layer with apparent energy activation of 235 kJ/mol. Temperature range (II) represents a transition range where the reductions were halted due to an accumulated lead layer.
- In the case of the current study, which can be extended to industrial practice, it appeared that in the case of pellet sample, the appropriate process parameters are reduced at 800 °C for at least 2 h to achieve the complete reduction.

The findings from the current study have ramification for industrial practice. Overall, the results from the current study suggest that hydrogen reduction of PbO to produce Pb is feasible. In industrial practice, however, it is vital to ensure that the lead droplets product is able to easily drain to allow the continuous reduction. Hence, a strategy for the arrangement of how the input PbO charge is distributed in the reactor (such as in blast furnace) will need to be carefully considered.

ACKNOWLEDGMENTS

The authors are grateful to Umicore Belgium and Swinburne University of Technology, Australia, for providing funding for the current study through joint SUPRA (Swinburne University Postgraduate Research Award) scholarship for PhD study of Asywendi Rukini.

FUNDING

Open Access funding enabled and organized by CAUL and its Member Institutions.

CONFLICT OF INTEREST

The authors declare that they have no conflict of interest.

OPEN ACCESS

REFERENCES

1. ILA (International Lead Association). Lead Production & Statistics. 2015. https://www.ila-lead.org/lead-facts/lead-production–statistics Accessed 10 Dec 2020.
2. U.B. Pal, T.D. Roy, and G. Simkovich: *Metall. Trans. B*, 1983, vol. 14B, pp. 693–701.
3. R.V. Culver, I.G. Matthew, and E.R.C. Spooner: *Aust. J. Chem.*, 1962, vol. 15, pp. 40–55.
4. I. Ricapito, C. Fazio, and G. Benamati: *J. Nuclear Mater.*, 2002, vol. 301, pp. 60–63.
5. I.I. Ivanov, V.M. Shelmet, V.V. Ulyanov, and Y.A. Teplyakov: *Kinet. Catal.*, 2015, vol. 56, pp. 304–307.
6. K.B. Blodgett: *J. Am. Ceram. Soc.*, 1951, vol. 34, pp. 14–27.
7. O.M. Kannunikova, F.Z. Gilmutdinov, and A.A. Shakov: *Int. J. Hydrogen Energy*, 2002, vol. 27, pp. 783–91.
8. H. Yonggang, Z. Yang, L. Hui, and G. Zhenan: *Proc. SPIE 8194, International Symposium on Photoelectronic Detection and Imaging 2011: Advances in Imaging Detectors and Applications*, 81941Q (18 August 2011). https://doi.org/10.1117/12.900283.
9. Y. Zhang, Y. Sun, J. Wang, K. Huang, Y. Wang, J. Liu, B. Zhang, W. Hou, and X. Lu: *IOP Conf. Ser.*, 2018, vol. 423, p. 012167.
10. G. Gallo: *Ann. Chim. Rome*, vol. 17, pp. 544–52.
11. J. Szekely, C.I. Lin, and H.Y. Sohn: *Chem. Eng. Sci.*, 1973, vol. 28(11), pp. 1975–89.
12. A. Khawam and D.R. Flanagan: *J. Phys. Chem. B*, 2006, vol. 100, pp. 17315–28.
13. H.S. Ray, S. Ray: *Chapter 11: Analysis of kinetics data for practical application, Kinetics of Metallurgical Processes*, 2018, pp. 315–39.
14. D. Pavlov: *Chapter 5 – Leady Oxide, A handbook of lead-acid battery technology and its influence on the product. Lead-Acid Batteries: Science and Technology (2nd Edition)*, 2017, pp 245–73.
15. D. Risold, J.I. Nagata, and R.O. Suzuki: *J. Phase Equilibria*, 1998, vol. 19, pp. 213–33.
16. K. Oka, H. Unoki, and T. Sakudo: *J. Crystal Growth*, 1979, vol. 47, pp. 568–72.
17. R. Soederquist and B. Dickens: *J. Phys. Chem. Solids*, 1967, vol. 28, p. 823.
18. T. W. Anthony. Method on operating a lead blast furnace. US Patent, 4219353A, 1980.
19. J. Lumsden. Lead blast furnace process. US Patent, 3243283, 1966.
20. V.I. Bolshakov: *Metallurgist*, 2010, vol. 54(3–4), pp. 153–57.
21. Y. Semenov, E.I. Shumel'chik, and V.V. Gorupakha: *Metallurgist*, 2018, vol. 61, pp. 950–58.
22. C. Yilmaz, J. Wendelstorf, and T. Turek: *J. Cleaner Prod.*, 2017, vol. 154, pp. 488–501.
23. H. Nogami, Y. Kashiwaya, and D. Yamada: *ISIJ Int.*, 2012, vol. 52(8), pp. 1523–27.
24. Q. Lyu, Y. Qie, X. Liu, C. Lan, J. Li, and S. Liu: *Thermochim. Acta*, 2017, vol. 648, pp. 79–90.

25. Y. Liu, Z. Hu, and Y. Shen: *Metall. Mater. Trans. B*, 2021, vol. 52(5), pp. 2971–91.
26. N. Barrett, S. Mitra, H. Doostmohammadi, D. O'dea, P. Zulli, S. Chew, and T. Honeyands: *ISIJ Int.*, 2022, vol. 62(6), pp. 1168–77.
27. F.A. Kanda and R.P. Colburn: *Phys. Chem. Liquids*, 1968, vol. 1:2, pp. 159–70. https://doi.org/10.1080/00319106808083795.
28. D.W.G. White: *Metall. Mater. Trans. B*, 1971, vol. 2B, pp. 3067–71. https://doi.org/10.1007/BF02814956.
29. E. Segal: *Rev. Roum. Chim.*, 2012, vol. 57(4–5), pp. 491–93.